https://doi.org/10.3311/PPee.37577

Periodica Polytechnica Electrical Engineering and Computer Science

Observer-based Implementation of Discrete Gabor Transform

Bence Ország[1*], László Sujbert[1]

[1] Department of Artificial Intelligence and Systems Engineering, Faculty of Electrical Engineering and Informatics, Budapest University of Technology and Economics, Műegyetem rkp. 3., H-1111 Budapest, Hungary
[*] Corresponding author, e-mail: orszag@mit.bme.hu

Received: 31 May 2024, Accepted: 18 December 2024, Published online: 17 January 2025

Abstract

The most commonly used technique in time-frequency analysis is the short-time Fourier transform. It can be used to determine the spectral components as they change over time by computing the Fourier transform of a windowed segment of the signal. A fundamental constraint of this method is that the frequency resolution of the representation in the time-frequency domain will be linear by design. The frequency adaptive nonstationary discrete Gabor transform offers an alternative that does not have this limitation. A Luenberger observer is capable of the implementation of the short-time Fourier transform, and its numerical advantages are already established based on the work of Hostetter and Péceli. Here, we introduce the family of discrete Gabor transforms and its properties along with a constructive method to define such transforms. Furthermore, we show that they are realizable by Luenberger observers which are capable of the error-free reconstruction of the observed signal in finite steps. The dead-beat property is derived for the state variables as well which estimate the transform of the windowed signal.

Keywords

observer, Gabor transform, frames, time-frequency representations

1 Introduction

Signal transforms play a key role in several digital signal processing algorithms. They can be used to highlight important signal characteristics. Virtually all signals are generated in the time domain, but their harmonic content is not readily apparent from that description of the signal. With the help of the Fourier transform, it can be transformed into the frequency domain. To preserve some of the time domain information, the short-time Fourier transform [1] and the Gabor transform [2] were developed.

The former can be implemented efficiently in a recursive manner with the help of an observer. This idea was first elaborated by Hostetter [3] and then by Péceli [4]. Since then, the field of the recursive discrete Fourier-transform has been well established [5, 6]. However, the resolution of the time-frequency plane cannot be adjusted with the granularity dictated by real-world applications. Therefore, a family of generalized Gabor transforms was developed based on frame theory [7] and successfully applied [8]. This paper gives a brief review of such transforms and as a novelty, it lays the theoretical foundations needed for the recursive implementation of them.

Sections 2 and 3 give the review of the necessary theory of frames and Gabor transforms, while Section 4 introduces the observer and the corresponding conceptual signal model and then proves that it is usable for the implementation of Gabor transforms. Section 4 also contains an example and illustrates the correctness. Section 5 details the computational benefits of the observer-based implementation compared to the naive FIR filter based one and proves asymptotic stability and the absence of limit cycles. Finally, Section 6 concludes the paper.

2 Frames

2.1 Definition

Signal transforms - like the Fourier transform - can be used to decompose a time domain signal into a weighted sum of components. The evaluation of the transform is nothing more than the computation of these weighting coefficients. A signal transform can be thought of as a pair of the set of components and the algorithm used to compute the weighting coefficients. The aforementioned set cannot be chosen freely, it needs to satisfy certain constraints, for example, to ensure that all elements of the time domain signal space can be expressed as a weighted sum.

Frame theory [9] is concerned with the study of signal transforms in the sense described above. In the general case,

Cite this article as: Ország, B., Sujbert, L. "Observer-based Implementation of Discrete Gabor Transform", Periodica Polytechnica Electrical Engineering and Computer Science, 2025. https://doi.org/10.3311/PPee.37577

the signals to be transformed are continuous and square-integrable. The remainder of this article will only discuss the discrete periodic case because this choice lets us use linear algebra to model the stated problems and it suits practical implementations, but the main result of the paper remains valid for nonperiodic signals as well. This means that the space of the signals is $\mathbb{C}^N$, while the set of the components used in the reconstruction is a subset of $\mathbb{C}^N$.

The elements of this set are called atoms denoted by $\boldsymbol{\varphi}_l$. If the signal to be reconstructed is $\boldsymbol{v} \in \mathbb{C}^N$, then

$$\boldsymbol{v} = \sum_{l=0}^{L-1} \alpha_l \boldsymbol{\varphi}_l, \tag{1}$$

where L is the total number of atoms and α_l is the weighting coefficient corresponding to the l^{th} atom. These atoms can be arranged into a $\mathbb{C}^{L\times N}$ matrix as row vectors

$$\boldsymbol{\Phi} = \begin{pmatrix} \boldsymbol{\varphi}_0 & \boldsymbol{\varphi}_1 & \cdots & \boldsymbol{\varphi}_{L-1} \end{pmatrix}^H. \tag{2}$$

Likewise, the α_l coefficients can be organized into a vector, so the sum in Eq. (1) can be rewritten in a compact form as

$$\boldsymbol{v} = \boldsymbol{\Phi}^H \boldsymbol{\alpha}. \tag{3}$$

An additional advantage of this notation is that it gives a hint for the computation of the weighting coefficients because

$$\boldsymbol{\alpha} = \left(\boldsymbol{\Phi}^H\right)^+ \boldsymbol{v}, \tag{4}$$

where $(\cdot)^+$ denotes the Moore-Penrose pseudoinverse. This choice leads to the

$$\boldsymbol{v} = \boldsymbol{\Phi}^H \boldsymbol{\alpha} = \boldsymbol{\Phi}^H \left(\boldsymbol{\Phi}^H\right)^+ \boldsymbol{v} = \boldsymbol{v} \tag{5}$$

identity, which might be true only if we have a right pseudoinverse. The condition for that to happen is the following. The rows of the $\boldsymbol{\Phi}$ matrix - the $\boldsymbol{\varphi}_l$ vectors - must span the space $\mathbb{C}^N$, so as a consequence $L \geq N$. Let's denote

$$\tilde{\boldsymbol{\Phi}} = \left(\boldsymbol{\Phi}^H\right)^+ = \boldsymbol{\Phi}\left(\boldsymbol{\Phi}^H\boldsymbol{\Phi}\right)^{-1} = \begin{pmatrix} \tilde{\boldsymbol{\varphi}}_0 & \tilde{\boldsymbol{\varphi}}_1 & \cdots & \tilde{\boldsymbol{\varphi}}_{L-1} \end{pmatrix}^H, \tag{6}$$

which is the matrix containing the so-called dual atoms. Using this new definition the dual atoms can be derived with the help of the atoms as

$$\tilde{\boldsymbol{\varphi}}_l = \left(\boldsymbol{\Phi}^H\boldsymbol{\Phi}\right)^{-1} \boldsymbol{\varphi}_l. \tag{7}$$

This leads to a more general definition of the computation of the weighting coefficients

$$\alpha[l] = \tilde{\boldsymbol{\varphi}}_l^H \boldsymbol{v} = \langle \boldsymbol{v}, \tilde{\boldsymbol{\varphi}}_l \rangle, \tag{8}$$

which can be substituted back into Eq. (1)

$$\boldsymbol{v} = \sum_{l=0}^{L-1} \langle \boldsymbol{v}, \tilde{\boldsymbol{\varphi}}_l \rangle \boldsymbol{\varphi}_l. \tag{9}$$

This form makes it apparent that the theory of frames intends to generalize the idea of bases. The weighting coefficients are the results of a projection, but not onto the "basis vector", but onto a dual. Knowing this, a frame can be defined as a matrix $\boldsymbol{\Phi}$ with a pseudoinverse $\tilde{\boldsymbol{\Phi}}$, which can be thought of as a transformation. In this sense, the evaluation of the transformation is the computation of the coefficients, while the inverse transformation is the weighted summation of the $\boldsymbol{\varphi}_l$ components. The matrix $\boldsymbol{\Phi}$ in itself is a frame candidate because if $(\boldsymbol{\Phi}^H\boldsymbol{\Phi})^{-1}$ exists, then $\tilde{\boldsymbol{\Phi}}$ can be computed.

2.2 Properties of frames

During the generalization of the notion of a basis, an important property is lost. As previously mentioned, $L \geq N$ must hold. If the inequality is strict, then the total number of atoms is larger than the dimension of the space they span, which leads to more than one expansion of the $\mathbf{0}$ signal because the $\boldsymbol{\varphi}_l$ atoms will be linearly dependent. This creates an ambiguity in the representations, by adding a nontrivial expansion of $\mathbf{0}$ to another set of coefficients, the value of the coefficients will change, but the sum weighted by them won't.

This problem can be resolved by observing that the coefficients are determined by the result of a projection (Eq. (8))

$$\boldsymbol{\alpha} = \tilde{\boldsymbol{\Phi}}\boldsymbol{v} = \tilde{\boldsymbol{\Phi}}\boldsymbol{\Phi}^H\boldsymbol{\beta} = \boldsymbol{P}\boldsymbol{\beta}, \tag{10}$$

where $\boldsymbol{\alpha}$ is the calculated expansion, and $\boldsymbol{\beta}$ is an arbitrary one. $\boldsymbol{P}$ is indeed a projection because by using Eq. (6)

$$\boldsymbol{P}^2 = \left(\tilde{\boldsymbol{\Phi}}\boldsymbol{\Phi}^H\right)^2 = \tilde{\boldsymbol{\Phi}}\left(\boldsymbol{\Phi}^H\tilde{\boldsymbol{\Phi}}\right)\boldsymbol{\Phi}^H = \tilde{\boldsymbol{\Phi}}\boldsymbol{\Phi}^H = \boldsymbol{P}. \tag{11}$$

This projection defines an N-dimensional subspace of $\mathbb{C}^L$. The coefficient vectors will be mapped into this subspace, which is the range of $\boldsymbol{P}$ by definition, whose basis can be calculated easily. Inside this subspace the reconstruction will be unambiguous. To prove it, first assume that it is ambiguous, which means that there exists $\boldsymbol{\alpha} \neq \boldsymbol{\beta}$ for which

$$\boldsymbol{v} = \boldsymbol{\Phi}^H\boldsymbol{\alpha} = \boldsymbol{\Phi}^H\boldsymbol{\beta} \tag{12}$$

holds. But because $\boldsymbol{\alpha}$ and $\boldsymbol{\beta}$ are in the subspace, the $\boldsymbol{P}$ projection will leave them unchanged, which leads to

$$\boldsymbol{\alpha} = \boldsymbol{P}\boldsymbol{\alpha} = \tilde{\boldsymbol{\Phi}}\boldsymbol{\Phi}^H\boldsymbol{\alpha} = \tilde{\boldsymbol{\Phi}}\boldsymbol{v} = \tilde{\boldsymbol{\Phi}}\boldsymbol{\Phi}^H\boldsymbol{\beta} = \boldsymbol{P}\boldsymbol{\beta} = \boldsymbol{\beta}. \tag{13}$$

But this is a contradiction, our initial assumption was false.

Duality is another important property of frames. It states that the roles of the atoms and dual atoms can be interchanged

$$\boldsymbol{v} = \sum_{l=0}^{L-1} \langle \boldsymbol{v}, \tilde{\boldsymbol{\varphi}}_l \rangle \boldsymbol{\varphi}_l = \boldsymbol{\Phi}^H \tilde{\boldsymbol{\Phi}} \boldsymbol{v} = \tilde{\boldsymbol{\Phi}}^H \boldsymbol{\Phi} \boldsymbol{v} = \sum_{l=0}^{L-1} \langle \boldsymbol{v}, \boldsymbol{\varphi}_l \rangle \tilde{\boldsymbol{\varphi}}_l . \tag{14}$$

The third equality holds as a consequence of Eq. (6), while the rest due to previous definitions. Later, this will prove useful because if we determine the dual atoms, we can calculate the atoms from them so that the design process can be executed in a reversed order.

3 Discrete Gabor transforms

Section 2.2 showed a general framework and assumed the existence of suitable atoms that can serve as a base for a frame. The goal is to present a constructive method that can generate the atoms for us based on a frequency domain specification. But before that, we give a concrete example of a frame that corresponds to the discrete Fourier transform.

3.1 Discrete Fourier transform

The unitary definition of the discrete Fourier transform is

$$\alpha[l] = \frac{1}{\sqrt{N}} \sum_{n=0}^{N-1} v[n] e^{-j\frac{2\pi}{N}ln} = \langle \boldsymbol{v}, \boldsymbol{f}_l \rangle, \tag{15}$$

which can be viewed as a scalar product. Based on this equivalence we can define the $\boldsymbol{\mathcal{F}} \in \mathbb{C}^{L\times N}$ matrix where $L = N$, and organize the transformed values into a vector

$$\boldsymbol{\alpha} = \boldsymbol{\mathcal{F}}\boldsymbol{v} = \begin{pmatrix} \boldsymbol{f}_0 & \boldsymbol{f}_1 & \cdots & \boldsymbol{f}_{L-1} \end{pmatrix}^H \boldsymbol{v}, \tag{16}$$

where

$$f_l[n] = \frac{1}{\sqrt{N}} e^{j\frac{2\pi}{N}ln}. \tag{17}$$

The inverse transform is

$$v[n] = \frac{1}{\sqrt{N}} \sum_{l=0}^{L-1} \alpha[l] e^{j\frac{2\pi}{N}nl} = \sum_{l=0}^{L-1} \langle \boldsymbol{v}, \boldsymbol{f}_l \rangle f_l[n]. \tag{18}$$

It is similar to Eq. (9), we can assert that the $\boldsymbol{f}_l$ vectors are good candidates to be atoms and dual atoms.

Considering Eq. (8) and Eq. (15), we can observe that they can be described mathematically in an identical way, but we interpreted them differently. By evaluating the scalar product, we computed the weighting coefficients in the first case, while in the second case, we computed one element of the signal transform. Likewise, there is a similarity between Eq. (9) and Eq. (18). This leads to a correspondence between transforms and frames. It's important to note, that this notion of transforms is not compatible with the one in linear algebra, but it helps us to define frames by transforms and vice versa and this is exactly what happens in Section 3.1. It only remains to show that the $\boldsymbol{f}_l$ vectors are the atoms and dual atoms, and this is indeed the case because

$$\tilde{\boldsymbol{f}}_l = \left(\boldsymbol{\mathcal{F}}^H \boldsymbol{\mathcal{F}}\right)^{-1} \boldsymbol{f}_l = \boldsymbol{f}_l, \; l = 0,\ldots,L-1. \tag{19}$$

In subsequent derivations, we will use the translation and modulation theorems of the Fourier transform, which can be summarized as

$$\boldsymbol{\mathcal{F}}\boldsymbol{T}_\tau = \boldsymbol{M}_{-\tau}\boldsymbol{\mathcal{F}}, \tag{20}$$

$$\boldsymbol{\mathcal{F}}\boldsymbol{M}_\omega = \boldsymbol{T}_\omega\boldsymbol{\mathcal{F}}, \tag{21}$$

where $\boldsymbol{T}_\tau$ is a circular time shift by τ, and $\boldsymbol{M}_\omega$ is a modulation by ω. Their definition for an arbitrary $\boldsymbol{v} \in \mathbb{C}^N$ is

$$\boldsymbol{T}_\tau v[n] = v\left[\operatorname{mod}(n-\tau, N)\right], \tag{22}$$

$$\boldsymbol{M}_\omega v[n] = v[n] e^{j\frac{2\pi}{N}\omega n}. \tag{23}$$

3.2 Discrete Gabor transform

The Fourier transform of a signal is a purely frequency domain representation, thus the time evolution of the frequency components is not readily apparent. The obvious solution to this problem is to partition the signal in the time domain into several segments and apply the Fourier transform to those.

By realizing that the segments can overlap one can define the short-time Fourier transform [1]. The Gabor transform [3] is a generalization of this idea. The result of the transform is a function of time and frequency, in the discrete case

$$\alpha[m,k] = \sum_{n=0}^{N-1} v[n] \overline{\phi[n-am]} e^{-j\frac{2\pi}{N}bkn} = \langle \boldsymbol{v}, \boldsymbol{M}_{bk}\boldsymbol{T}_{am}\boldsymbol{\phi} \rangle. \tag{24}$$

The $\phi[n]$ window function is slid over the signal in steps determined by the a time hop parameter, which means $m = 0, \ldots, N/a - 1$. Then, the discrete Fourier transform is computed for every b^{th} frequency, so $k = 0, \ldots, N/b - 1$. Consequently, the total number of α coefficients is

$$L = \frac{N^2}{ab}. \tag{25}$$

As a remark, by choosing $a = b = 1$ we get the short-time Fourier transform as a special case when the coefficient number is maximal. Fig. 1 illustrates the meaning of the m and k indices. They can be used to specify a point in the time-frequency plane, where the set of possible points - which has cardinality L - can be seen in Fig. 1. It is called a sampling grid because it samples the time-frequency plane in the sense explained in the following paragraphs.

First, we need to assert some properties of this plane, considering that we have constrained the signals to be discrete and periodic. Due to the discretization the time axis will be discrete, and the frequency axis will be periodic, and due to the periodicity, the time axis will be periodic and the frequency axis discrete. This means that both the time and frequency axes are discrete and periodic. If the axes of Fig. 1 are scaled in a way that the period is N both in time and frequency, then the discrete points are exactly the integers $0, \ldots, N-1$.

One could assume that we would have a perfect understanding of the signal's behavior in both domains if we knew all N^2 points of the plane. To compute them, we could use a short-time Fourier transform with a window function that has a support small enough on the time-frequency plane to filter out all but one point of the signal, let's say at (m^*,k^*). Unfortunately, the Gabor uncertainty principle states that the window cannot be perfectly localized in time and frequency simultaneously. In practical terms, multiple points of the plane will affect the computation of the sought-after signal component. If the window function is chosen well, then these points will be localized around (m^*,k^*), which means that neighboring coefficients will be dependent.

This dependence introduces redundancy into the signal representation, and by increasing a and b, it can be reduced. In Fig. 1 the window function is better localized in time than in frequency, which means that the dependence will be larger in the frequency domain, so we can skip more samples there. It's worth mentioning that sampling is not mandatory but beneficial because we can save computational resources without losing information about the signal. But this raises the question of how large a and b can be. If the transform defined in Eq. (24) is invertible that means we have a complete description of the signal.

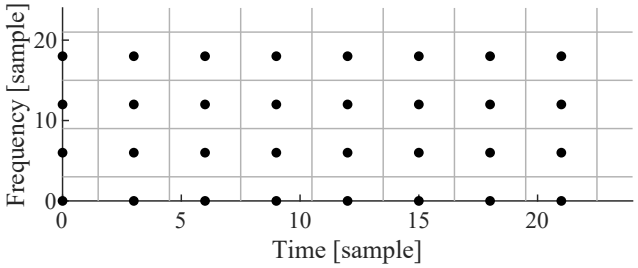

Fig. 1 Example sampling grid of the time-frequency plane for a Gabor transform when $N = 24$, $a = 3$, $b = 6$, and $L = 32$. The gray boxes visualize the supports of the ideal translated and modulated windows corresponding to the transform coefficients inside them.

To investigate invertibility, first we need to organize the $\alpha[m,k]$ coefficients into a $\mathbb{C}^L$ vector. By choosing a row-major order, the linear index is

$$l = m + \frac{N}{a}k. \tag{26}$$

Likewise, with this ordering the translated and modulated window functions can be organized into a matrix. These can be thought of as the dual atoms of a frame. By using duality (Eq. (14)), the existence of the atoms can be checked with Eq. (6), which proves the invertibility of the transform, but a more practical set of conditions can be given with a further generalization.

3.3 Nonstationary discrete Gabor transform

Section 3.2 presented the family of Gabor transforms. Fig. 1 illustrates that all transforms from this family have a linear temporal and frequency resolution, i.e. the samples are equally spaced. This is by design, the exact distances are a and b, respectively.

By choosing the transform to be

$$\alpha[m,k] = \sum_{n=0}^{N-1} v[n]\overline{\phi_k[n - a_k m]} = \langle \boldsymbol{v}, \boldsymbol{T}_{a_k m}\boldsymbol{\phi}_k \rangle, \tag{27}$$

that is, we have K distinct $\phi_k[n]$ window functions and corresponding a_k time hop parameters. This way the modulation is essentially built into the window, so the frequency axis is partitioned by them into potentially nonlinearly distributed domains. The a_k parameters should be chosen to be integers, but N/a_k must also be an integer. By choosing the window functions to be the modulation of $\phi[n]$ and setting $a_k = a$ for all k, we get back Eq. (24), so the new transform is indeed a generalization of the Gabor transform, called the frequency adaptive nonstationary Gabor transform [7].

In the frame theoretic interpretation of the transform we have the atoms in the form

$$\boldsymbol{\varphi}_l = \boldsymbol{T}_{a_k m}\boldsymbol{\phi}_k, \tag{28}$$

where $k = 0, \ldots, K-1$ and $m = 0, \ldots, N/a_k - 1$, so

$$L = \sum_{k=0}^{K-1} \frac{N}{a_k} \tag{29}$$

is the total number of atoms. The linear l index is given by

$$l = m + \sum_{i=0}^{k-1} \frac{N}{a_k}. \tag{30}$$

So, the matrix containing the atoms takes the form

$$\boldsymbol{\Phi} = \begin{pmatrix} \boldsymbol{\phi}_0 & \boldsymbol{T}_{a_0}\boldsymbol{\phi}_0 & \cdots & \boldsymbol{T}_{N-a_0}\boldsymbol{\phi}_0 & \boldsymbol{\phi}_1 & \cdots & \boldsymbol{T}_{N-a_k}\boldsymbol{\phi}_{a_k} \end{pmatrix}^H. \tag{31}$$

3.4 Proof of invertibility

Section 3.4 states the precise conditions for the invertibility of the nonstationary Gabor transform and then proves it [10].

Let the $\boldsymbol{\varphi}_l$ atoms of the frame be generated by the $\boldsymbol{\phi}_k$ prototype atoms like in Eq. (28). If the lengths of the supports of $\boldsymbol{\mathcal{F}}\boldsymbol{\phi}_k$ are finite with values $N_k \leq N$ and $a_k \leq N/N_k$ such that a_k and N/a_k are integers, and for all $n = 0, \ldots, N-1$

$$S[n] = \sum_{k=0}^{K-1} \frac{N}{a_k} \left| (\boldsymbol{\mathcal{F}}\boldsymbol{\phi}_k)[n] \right|^2 > 0 \tag{32}$$

then the dual atoms exist, so the transform is invertible.

The outline of the proof is the following. First, we introduce an auxiliary frame candidate $\boldsymbol{\Psi}$ which is a frame if and only if $\boldsymbol{\Phi}$ is. We show that $\boldsymbol{\Psi}$ is a frame by inverting $\boldsymbol{\Psi}^H\boldsymbol{\Psi}$ and by computing it's dual atoms using Eq. (7), which in turn can be used to determine the $\tilde{\boldsymbol{\varphi}}_l$ dual atoms. By showing the existence of these, we prove the invertibility of the transform.

Let's introduce auxiliary prototypes as

$$\boldsymbol{\psi}_k = \boldsymbol{\mathcal{F}}\boldsymbol{\phi}_k. \tag{33}$$

An auxiliary frame can be derived with Eq. (20) as

$$\boldsymbol{\Psi} = \boldsymbol{\Phi}\boldsymbol{\mathcal{F}}^H = \begin{pmatrix} \boldsymbol{\psi}_0 & \boldsymbol{M}_{-a_0}\boldsymbol{\psi}_0 & \cdots & \boldsymbol{M}_{-N+a_k}\boldsymbol{\psi}_{a_k} \end{pmatrix}^H, \tag{34}$$

and this leads to

$$\begin{aligned} \left(\boldsymbol{\Phi}^H\boldsymbol{\Phi}\right)^{-1} &= \boldsymbol{\mathcal{F}}^H\boldsymbol{\mathcal{F}}\left(\boldsymbol{\Phi}^H\boldsymbol{\Phi}\right)^{-1}\boldsymbol{\mathcal{F}}^H\boldsymbol{\mathcal{F}} \\ &= \boldsymbol{\mathcal{F}}^H\left(\boldsymbol{\mathcal{F}}\boldsymbol{\Phi}^H\boldsymbol{\Phi}\boldsymbol{\mathcal{F}}^H\right)^{-1}\boldsymbol{\mathcal{F}} = \boldsymbol{\mathcal{F}}^H\left(\boldsymbol{\Psi}^H\boldsymbol{\Psi}\right)^{-1}\boldsymbol{\mathcal{F}} \end{aligned} \tag{35}$$

as a consequence, which means that $\boldsymbol{\Phi}^H\boldsymbol{\Phi}$ is invertible if and only if $\boldsymbol{\Psi}^H\boldsymbol{\Psi}$ is. So, by computing $(\boldsymbol{\Psi}^H\boldsymbol{\Psi})^{-1}$, we can calculate the $\tilde{\boldsymbol{\varphi}}_l$ dual atoms. This matrix will be diagonal:

$$\begin{aligned} \left(\boldsymbol{\Psi}^H\boldsymbol{\Psi}\right)[p,q] &= \sum_{k=0}^{K-1} \psi_k[p]\overline{\psi_k[q]} \sum_{m=0}^{\frac{N}{a_k}-1} e^{j\frac{2\pi}{N}a_k m(p-q)} \\ &= \sum_{k=0}^{K-1} \psi_k[p]\overline{\psi_k[q]} \frac{N}{a_k} \delta\left[\operatorname{mod}\left(p-q, \frac{N}{a_k}\right)\right]. \end{aligned} \tag{36}$$

The first equality uses the definitions Eq. (34) and Eq. (23), while the second can be derived with the formula of the sum of finite terms of a geometric series. The $\delta[n]$ denotes the unit impulse, so the sum depends only on a_k and $\boldsymbol{\psi}_k$. For the off-diagonal elements, there are two cases. If the impulse is zero, then the sum is zero as well, but when the impulse is not zero, then the sum will be zero because in that case $|p-q| \geq N_k \leq N/a_k$, so either $\psi_k[p]$ or $\psi_k[q]$ or both will lie outside of the support of $\boldsymbol{\psi}_k$. But this result means that $\boldsymbol{\Psi}^H\boldsymbol{\Psi}$ is diagonal, with elements $S[n]$ on the diagonal. Due to Eq. (32), they will be nonzero, so the inverse is a diagonal matrix with elements $S^{-1}[n]$.

Based on Eq. (7) and Eq. (28) the dual atoms are

$$\begin{aligned} \tilde{\boldsymbol{\varphi}}_l &= \left(\boldsymbol{\Phi}^H\boldsymbol{\Phi}\right)^{-1}\boldsymbol{T}_{a_k m}\boldsymbol{\phi}_k = \boldsymbol{\mathcal{F}}^H\left(\boldsymbol{\Psi}^H\boldsymbol{\Psi}\right)^{-1}\boldsymbol{M}_{-a_k m}\boldsymbol{\mathcal{F}}\boldsymbol{\phi}_k \\ &= \boldsymbol{\mathcal{F}}^H\boldsymbol{M}_{-a_k m}\left(\boldsymbol{\Psi}^H\boldsymbol{\Psi}\right)^{-1}\boldsymbol{\mathcal{F}}\boldsymbol{\phi}_k = \boldsymbol{T}_{a_k m}\tilde{\boldsymbol{\phi}}_k. \end{aligned} \tag{37}$$

The derivations use the translation and modulation theorems (Eq. (20) and Eq. (21)) throughout. The third equality is explainable using the definition of the modulation operator and the fact that the inverse is diagonal. This result means that the dual atoms are generated by the duals of the prototypes, but by definition they are the inverse Fourier transform of the dual auxiliary prototypes, so

$$\left(\boldsymbol{\mathcal{F}}\tilde{\boldsymbol{\phi}}_k\right)[n] = \frac{\psi_k[n]}{S[n]} = \frac{(\boldsymbol{\mathcal{F}}\boldsymbol{\phi}_k)[n]}{\sum_{i=0}^{K-1} \frac{N}{a_i} \left|(\boldsymbol{\mathcal{F}}\boldsymbol{\phi}_i)[n]\right|^2}. \tag{38}$$

But by this, we have concluded the proof.

3.5 Useful properties

By observing Eq. (38), it is apparent that $S[n]$ is a non-negative real function. The dual atoms are identical to the atoms, if for all n

$$S[n] = 1. \tag{39}$$

But this can always be ensured with proper normalization if Eq. (32) holds. This is a useful property because in a practical implementation the memory requirements can be halved. Another advantage is that

$$\boldsymbol{\Psi}^H\boldsymbol{\Psi} = \boldsymbol{\Phi}^H\boldsymbol{\Phi} = \boldsymbol{I} \tag{40}$$

by definition which means that the Parseval identity holds for the frame [9], which states the equality of the time and in this case the time-frequency representation's energy, i.e.

$$\sum_{n=0}^{N-1} |v[n]|^2 = \sum_{k=0}^{K-1} \sum_{m=0}^{\frac{N}{a_k}-1} |\alpha[m,k]|^2. \tag{41}$$

If we define

$$\psi_k[n] = \frac{\chi_k[n]}{\sqrt{\sum_{i=0}^{K-1} \frac{N}{a_i} |\chi_i[n]|^2}}, \tag{42}$$

where $\boldsymbol{\chi}_k$ are prototype atoms satisfying the invertibility conditions, then we can prove that Eq. (40) holds because

$$\left(\Psi^H \Psi\right)[n,n] = \sum_{k=0}^{K-1} \frac{N}{a_k} |\psi_k[n]|^2 = \frac{\sum_{k=0}^{K-1} \frac{N}{a_k} |\chi_k[n]|^2}{\sum_{k=0}^{K-1} \frac{N}{a_i} |\chi_i[n]|^2} = 1. \tag{43}$$

There is another useful condition that can be used to constrain the L number of atoms. It was stated previously that for a frame $L \geq N$ always holds, but if the biorthogonality condition [11] can be satisfied, then $L = N$. It can be derived from Eq. (29) by dividing both sides by N so

$$\sum_{k=0}^{K-1} \frac{1}{a_k} = 1. \tag{44}$$

In this case, the number of atoms is definitionally equal to the dimension of the signal space, and they span it as well, so they form a basis of $\mathbb{C}^N$. This will be true for the dual atoms as well and they will form a biorthogonal basis. This makes the signal representation unambiguous, but it has the practical benefit of reducing the necessary computational resources by minimizing the number of atoms. It must be noted that this is a quite restrictive constraint because a_k and N/a_k need to be integers.

3.6 Examples

A wide range of transforms can be designed by the introduction of the nonstationary Gabor transform. The simplest of these, from a mathematical standpoint, is the identity which gives the original signal as a result. It can be acquired by setting $K = 1$, $a_0 = 1$ and $\boldsymbol{\phi}_0 = \boldsymbol{e}_0$ which is the first standard basis vector. Trivially, $L = N$ and the dual atoms are equal to the atoms. The Fourier transform of $\boldsymbol{e}_0$ is a constant, so it is not localized in frequency at all.

The first nontrivial example is the Fourier transform as a special case. The parameters should be $K = N$, $a_k = N$ and $\boldsymbol{\psi}_k = \boldsymbol{e}_k$, so the $\boldsymbol{\phi}_k$ prototypes will be complex exponentials. The choice of a_k ensures that $L = N$. The equality of the atoms and the dual atoms holds by definition.

The main example is a general nonstationary Gabor transform. The frequency domain specifications of the atoms are given by $\mathcal{F}\boldsymbol{\phi}_k$ shown in Fig. 2, while the resulting atoms and the sampling grid in Fig. 3 and Fig. 4

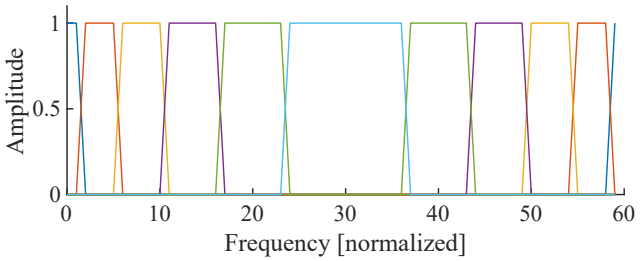

Fig. 2 Frequency domain specification of $K = 10$ window functions for the example. The ones forming complex conjugate pairs have the same color.

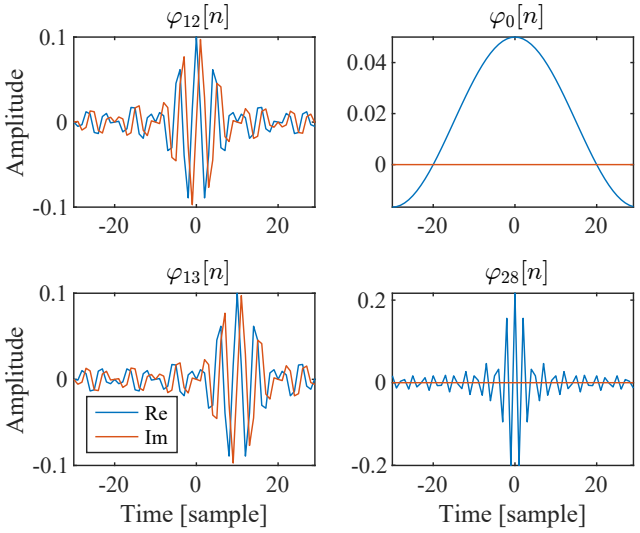

Fig. 3 The value of some of the atoms in the example

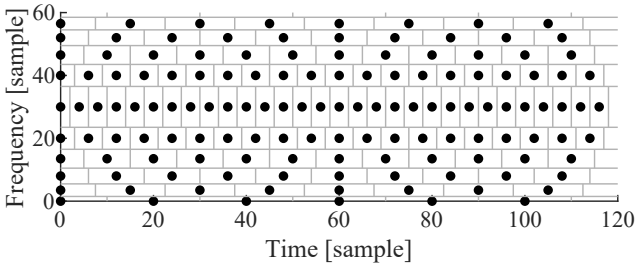

Fig. 4 The sampling grid of the time-frequency plane in the example. Note that $N = 60$ so two identical periods can be seen in time, the second starts at $n = 60$.

respectively. The center frequencies of the specified window functions lie exactly on the sampling points. To satisfy Eq. (32), hence invertibility, the value of the a_k time hop parameters should be chosen as the largest integer less than the support of $\mathcal{F}\boldsymbol{\phi}_k$, while ensuring that N/a_k is an integer. This is the number of samples that correspond to a frequency band in Fig. 4. They can be calculated with the atoms depicted in Fig. 3 which refers to them with their linear indices. The $\varphi_0[n]$ corresponds to the symmetrical frequency region around 0, so its value is real, while for a similar reason $\varphi_{28}[n]$ is also real. Their support in the time domain is not finite but they are localized. The remaining

two atoms are only different by a translation, and it can be seen that their approximate supports overlap, which means that this frequency region's neighboring samples in the time-frequency plane will be dependent. Another thing to note is that the samples form complex conjugate pairs, so if the transformed signal is real, then the coefficients corresponding to these pairs will be each other's conjugates. This can be used in a practical implementation, only half of the coefficients must be computed, and the other half can be inferred using this fact.

4 Common structure for recursive discrete transforms

Section 4 introduces the Luenberger observer [3, 4] and a linear model whose state is estimated by the former. The presentation of the theory is based on [11]. As a novelty, it is proved that the observer implementing a frame-induced transform is capable of the error-free reconstruction of the observed signal in finite steps. In the case when the signal is periodic, then the dead-beat property is derived for the state variables as well, and they will be an optimal approximation of the true set of weighting coefficients in a quadratic sense.

4.1 Conceptual signal model

The conceptual signal model [4] is a linear system whose $y[n]$ output is acquired by the summation of the $\varphi_l[n]$ atoms weighted by the $x_l[n]$ state variables. The total number of atoms is L. They are periodic by definition with period N and their values are given on the $n = 0, \ldots, N-1$ timesteps so for any $n \in \mathbb{Z}$

$$\varphi_l[n] = \varphi_l[\operatorname{mod}(n, N)], \tag{45}$$

and the values of the atoms at n collected into a vector is

$$\boldsymbol{\varphi}[n] = \boldsymbol{\Phi}\boldsymbol{e}[n] = \begin{pmatrix}\varphi_0[n] & \varphi_1[n] & \cdots & \varphi_{L-1}[n]\end{pmatrix}^H, \tag{46}$$

where $\boldsymbol{e}[n]$ is the n^{th} standard basis vector. Both of the above are assumed for all signals introduced later, with the notable exception of $y[n]$, which might be nonperiodic.

The output of the signal model can be calculated as

$$y[n] = \boldsymbol{\varphi}^H[n]\boldsymbol{x}[n]. \tag{47}$$

For the periodic case, the values of the state variables are constant, but in the case they are not, then every possible $y[n]$ discrete signal is constructable [11] by choosing

$$\boldsymbol{x}[n] = \tilde{\boldsymbol{\varphi}}[n]y[n] \tag{48}$$

because by assuming that the atoms form a frame, then

$$y[n] = \boldsymbol{\varphi}^H[n]\boldsymbol{x}[n] = \boldsymbol{e}^H[n]\boldsymbol{\Phi}^H\tilde{\boldsymbol{\Phi}}\boldsymbol{e}[n]y[n] = y[n] \tag{49}$$

which is a consequence of Eq. (6).

4.2 Observer

The state variables of the described signal model can be estimated by a properly designed observer which was introduced and analyzed in [4]. This can be seen in Fig. 5. It tries to reconstruct the $y[n]$ input signal by refining the $\hat{\boldsymbol{x}}[n]$ estimated state variables based on the $\varepsilon[n]$ estimation error with the help of the $\tilde{\varphi}_l[n]$ dual atoms. The time course of the estimated state variables can be given by

$$\begin{aligned}\hat{\boldsymbol{x}}[n+1] &= \hat{\boldsymbol{x}}[n] + \tilde{\boldsymbol{\varphi}}[n]\boldsymbol{\varphi}^H[n]\left(\boldsymbol{x}[n] - \hat{\boldsymbol{x}}[n]\right) \\ &= \left(\boldsymbol{I} - \tilde{\boldsymbol{\varphi}}[n]\boldsymbol{\varphi}^H[n]\right)\hat{\boldsymbol{x}}[n] + \tilde{\boldsymbol{\varphi}}[n]y[n].\end{aligned} \tag{50}$$

It was proven in [4] that $\hat{\boldsymbol{x}}[n] = \boldsymbol{x}[0]$ after N time steps (or less) if $\tilde{\boldsymbol{\varphi}}[n]$ and $\boldsymbol{\varphi}[n]$ form a biorthogonal basis and the state variables of the conceptual signal model are constant. We can generalize this result by showing that the statement remains valid if $\tilde{\boldsymbol{\varphi}}[n]$ and $\boldsymbol{\varphi}[n]$ form a frame.

The repeated application of the state equation results in

$$\begin{aligned}\hat{\boldsymbol{x}}[n] &= \left(\prod_{i=0}^{n-1}\left(\boldsymbol{I} - \tilde{\boldsymbol{\varphi}}[i]\boldsymbol{\varphi}^H[i]\right)\right)\hat{\boldsymbol{x}}[n] \\ &+ \sum_{j=0}^{n-1}\left(\prod_{i=j+1}^{n-1}\left(\boldsymbol{I} - \tilde{\boldsymbol{\varphi}}[i]\boldsymbol{\varphi}^H[i]\right)\right)\tilde{\boldsymbol{\varphi}}[j]y[j].\end{aligned} \tag{51}$$

In extreme cases, when the upper index in a sum or product is less than the lower, then the result is 0 or 1. Note that the periodic extension of the signals (Eq. (45)) will be used throughout the proof. First, we will prove that after N timesteps, the initial condition of the estimated state variable won't affect the estimation. This enables the

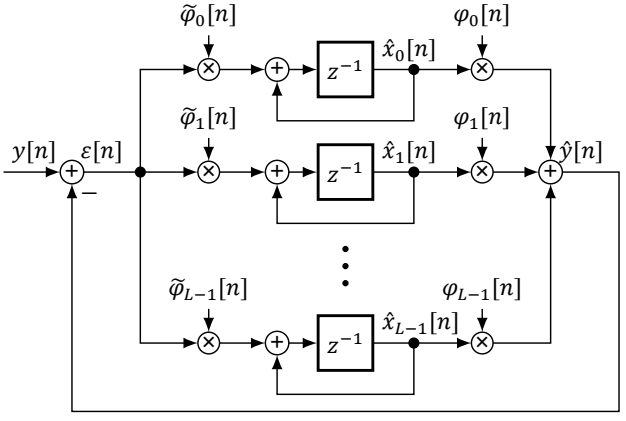

Fig. 5 An observer for recursive transformations

simplification of Eq. (51), which can be used to conclude that the estimation error is zero.

The initial condition affects the estimation at N through

$$\prod_{i=0}^{N-1}\left(\boldsymbol{I}-\tilde{\boldsymbol{\varphi}}[i]\boldsymbol{\varphi}^H[i]\right)=\boldsymbol{I}-\sum_{i=0}^{N-1}\tilde{\boldsymbol{\varphi}}[i]\boldsymbol{\varphi}^H[i]$$
$$=\boldsymbol{I}-\tilde{\boldsymbol{\Phi}}\left(\sum_{i=0}^{N-1}\boldsymbol{e}[i]\boldsymbol{e}^H[i]\right)\boldsymbol{\Phi}^H=\boldsymbol{I}-\tilde{\boldsymbol{\Phi}}\boldsymbol{\Phi}^H. \tag{52}$$

In the second equality only definitions, while in the third the dyadic decomposition of the identity matrix is used. The first equality holds because during the expansion of the product when $i \neq j$ the resulting term is

$$\tilde{\boldsymbol{\varphi}}[i]\boldsymbol{\varphi}^H[i]\tilde{\boldsymbol{\varphi}}[j]\boldsymbol{\varphi}^H[j]=\tilde{\boldsymbol{\varphi}}[i]\boldsymbol{e}^H[i]\boldsymbol{\Phi}^H\tilde{\boldsymbol{\Phi}}\boldsymbol{e}[j]\boldsymbol{\varphi}^H[j]=\boldsymbol{0} \tag{53}$$

because of Eq. (6) and because the scalar product of different standard basis vectors is zero. But the result of Eq. (52) is an orthogonal complementary projection of the one in Eq. (10)

$$\left(\boldsymbol{I}-\tilde{\boldsymbol{\Phi}}\boldsymbol{\Phi}^H\right)\tilde{\boldsymbol{\Phi}}\boldsymbol{\Phi}^H=\tilde{\boldsymbol{\Phi}}\boldsymbol{\Phi}^H-\tilde{\boldsymbol{\Phi}}\boldsymbol{\Phi}^H=\boldsymbol{0}. \tag{54}$$

So, for all $n \geq N$ the estimation is independent from the initial value, assuming that it is in the subspace of the $\tilde{\boldsymbol{\Phi}}\boldsymbol{\Phi}^H$ projection because the orthogonal projection will map these elements to zero. Zero is suitable to be the initial condition because it is an element of all subspaces.

Based on the previous idea, it can be shown that the estimation will be independent of $y[j]$ if $j < n - N$, in other words, only the last N values of the input affect the estimation. Using these Eq. (50) can be simplified

$$\hat{\boldsymbol{x}}[n]=\sum_{j=n-N}^{n-1}\left(\boldsymbol{I}-\sum_{i=j+1}^{n-1}\tilde{\boldsymbol{\varphi}}[i]\boldsymbol{\varphi}^H[i]\right)\tilde{\boldsymbol{\varphi}}[j]\boldsymbol{\varphi}^H[j]\boldsymbol{x}[j]$$
$$=\sum_{i=n-N}^{n-1}\tilde{\boldsymbol{\varphi}}[i]\boldsymbol{\varphi}^H[i]\boldsymbol{x}[i]=\sum_{i=n-N}^{n-1}\tilde{\boldsymbol{\varphi}}[i]y[i]. \tag{55}$$

To assert the validity of the second equality, some consideration is needed. By multiplying with $\tilde{\boldsymbol{\varphi}}[j]\boldsymbol{\varphi}^H[j]$ from the right Eq. (53) is always applicable due to the definition of i.

From the estimated state the estimated output is

$$\hat{y}[n]=\sum_{i=n-N}^{n-1}\boldsymbol{e}^H[n]\boldsymbol{\Phi}^H\tilde{\boldsymbol{\Phi}}\boldsymbol{e}[i]y[i]=y[n-N], \tag{56}$$

where the first equality is the direct consequence of the previous result while the second is true due to Eq. (6) and because $\boldsymbol{e}^H[n]\boldsymbol{e}[i] = 1$ only if $i = n - N$. This proves that the observer can reconstruct an arbitrary $y[n]$ signal without errors. Finally, the estimation error is

$$\varepsilon[n]=y[n]-\hat{y}[n]=\boldsymbol{\varphi}^H[n]\left(\boldsymbol{x}[n]-\sum_{i=n-N}^{n-1}\tilde{\boldsymbol{\varphi}}[i]\boldsymbol{\varphi}^H[i]\boldsymbol{x}[i]\right). \tag{57}$$

This means $\varepsilon[n]$ will exactly be zero without delay only when $y[n]$ is periodic with period N, which is ensured if $\boldsymbol{x}[n]$ is constant. In that case, it can be factored out from the right, so we are left with Eq. (52). If $\boldsymbol{x}[0]$ was in the subspace of the projection, then $\hat{\boldsymbol{x}}[n] = \boldsymbol{x}[0]$. Otherwise, there will be a constant error. This result concludes the proof.

4.3 Example

The main example presented in Section 3.6 can be implemented by the observer, so the atoms are the ones depicted in Fig. 3. Consequently, the values of the $\hat{x}_l[n]$ state variables correspond to the $\alpha[m,k]$ coefficients, the connection between the indices is given by Eq. (30). This can be used to interpret the state variables as a sampling of the time-frequency plane like in Fig. 4. Because of Eq. (55) only the last N samples of $y[n]$ is taken into account in the estimation, $\hat{\boldsymbol{x}}[n]$ contains the transform of the periodic extension of these N values, resulting in a so-called sliding window method.

Stepping the time by one moves all of the sampling points of the time-frequency plane by one as well. If the observer implements a discrete Fourier transform, then the state variables take on the values of the short-time Fourier transform of the signal. But this is not the case in general. On every N^{th} timestep the sampling points will align as on Fig. 4. To interpret $\hat{\boldsymbol{x}}[n]$ as a sampling of the time-frequency plane, we need to consider it only every N^{th} timestep.

In Fig. 6, the output of the observer can be seen for a noncoherently sampled sawtooth wave. The input is delayed by N, so it can be verified that the output is indeed equal to it. The difference of the two is plotted in Fig. 7. The error drops to virtually zero after N timesteps, the remaining error is due to the machine precision of 64-bit floating point operations. This validates the theory, Eq. (56) in particular.

5 Computational and numerical properties

The added complexity of the observer-based implementation results in several advantageous properties. Section 5 details some of these while comparing them to the naive

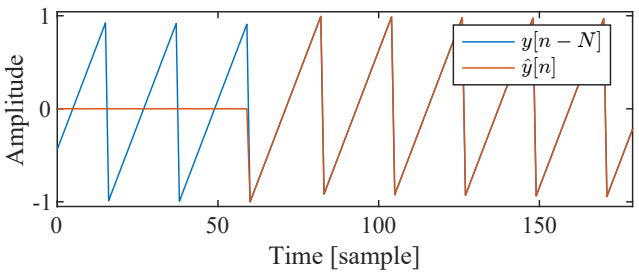

Fig. 6 The delayed input and the output of the observer

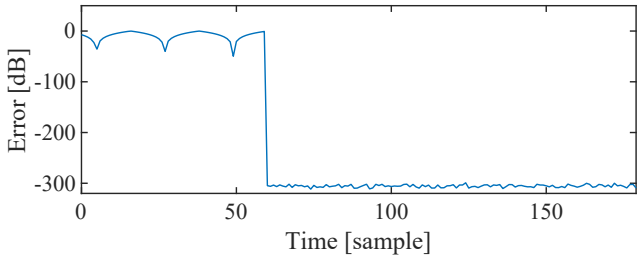

Fig. 7 The error of the reconstruction for the example

FIR filter based implementation of the discrete Gabor transform. The latter can be obtained by inspecting Eq. (9) and realizing that the scalar product can be evaluated as a convolution. If the components of the signal to be transformed are stored in a delay line of a FIR filter then the output of the filter will coincide with a transform coefficient corresponding to one of the atoms. Fig. 8 illustrates how to implement the transform based on this approach. The $\boldsymbol{\varphi}(z)$ and $\tilde{\boldsymbol{\varphi}}(z)$ transfer functions are polynomials of z having the corresponding (dual) atoms' components as coefficients.

5.1 Computational complexity

In the case where the transform of the input signal is to be processed in a sliding window manner, then the observer can operate with significantly less resources. In order to keep the notation consistent with Sections 2–4, we denote the length of the impulse responses of the FIR filters by N and the number of filters by L. Based on Fig. 5 and Fig. 8, we can determine the necessary computational resources and give a quantitative comparison between the implementation methods [6]. This is summarized by Table 1 and it clearly shows that the necessary amount of working memory and the number of multiplications can be reduced. This is due to the continuous operation of the observer, which distributes the operational load between the samples by the means of the feedback.

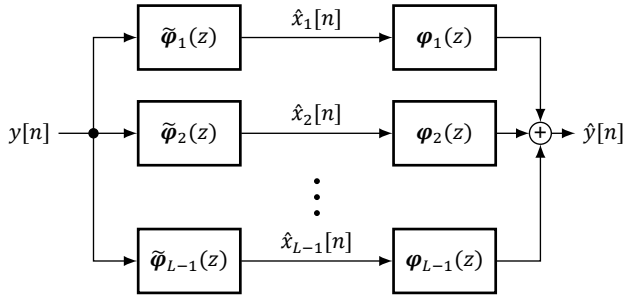

Fig. 8 FIR-based implementation of discrete Gabor transforms

Table 1 Complexity comparison of FIR and observer-based implementations

	Memory		Mult.	Adders	
Type	ROM	RAM		2-input	N-input
FIR	$2NL$	$(L+1)(N-1)$	$2NL$	0	$2L+1$
Obs.	$2NL$	L	$2N$	$L+1$	1

It's important to note that the number representation is assumed to be complex. This means that the values contained in Table 1 cannot be directly interpreted as the necessary number of hardware resources, it is only indicative of it.

5.2 Numerical stability

To assess the issue of stability, we can examine how the norm of the state variable vector changes over time in relation to the inputs and outputs. The proof of asymptotic stability [12] starts by sorting Eq. (50) and Eq. (47) into a vector,

$$\begin{pmatrix} \hat{\boldsymbol{x}}[n+1] \\ \hat{y}[n] \end{pmatrix} = \underbrace{\begin{pmatrix} \boldsymbol{I}-\tilde{\boldsymbol{\varphi}}[n]\boldsymbol{\varphi}^H[n] & \tilde{\boldsymbol{\varphi}}[n] \\ \boldsymbol{\varphi}^H[n] & 0 \end{pmatrix}}_{\boldsymbol{T}} \begin{pmatrix} \hat{\boldsymbol{x}}[n] \\ y[n] \end{pmatrix}. \tag{58}$$

Then we can compute the scalar product of each side of the equation with itself to get the square of the norms we seek,

$$\begin{pmatrix} \hat{\boldsymbol{x}}[n+1] \\ \hat{y}[n] \end{pmatrix}^H \begin{pmatrix} \hat{\boldsymbol{x}}[n+1] \\ \hat{y}[n] \end{pmatrix} = \begin{pmatrix} \hat{\boldsymbol{x}}[n] \\ y[n] \end{pmatrix}^H \boldsymbol{T}^H\boldsymbol{T} \begin{pmatrix} \hat{\boldsymbol{x}}[n] \\ y[n] \end{pmatrix}. \tag{59}$$

The only part of the equation that can be simplified is

$$\boldsymbol{T}^H\boldsymbol{T} = \begin{pmatrix} \boldsymbol{I}+2\boldsymbol{\varphi}[n]\boldsymbol{\varphi}^H[n] & \tilde{\boldsymbol{\varphi}}[n]-\boldsymbol{\varphi}[n] \\ -\boldsymbol{\varphi}[n]\tilde{\boldsymbol{\varphi}}^H[n]-\tilde{\boldsymbol{\varphi}}[n]\boldsymbol{\varphi}^H[n] & \\ \tilde{\boldsymbol{\varphi}}^H[n]-\boldsymbol{\varphi}^H[n] & 1 \end{pmatrix}. \tag{60}$$

If Eq. (39) holds, then $\tilde{\boldsymbol{\varphi}}[n] = \boldsymbol{\varphi}[n]$ so $\boldsymbol{T}^H\boldsymbol{T} = \boldsymbol{I}$, which proves the orthogonality of the structure and results in

$$\sum_{k=0}^{K-1}\hat{\boldsymbol{x}}^2[n+1]-\sum_{k=0}^{K-1}\hat{\boldsymbol{x}}^2[n] = u^2[n]-y^2[n]. \tag{61}$$

When $u[n] = 0$, then the norm of the state vector will always decrease, which leads to asymptotic stability by definition. Furthermore, the absence of limit cycles is guaranteed if we choose magnitude truncation during quantization.

6 Conclusion

The paper first established the theory of frames and some of the important results. This was followed by a detailed description of the Gabor transform and its generalization, which has adaptivity in the frequency domain. The invertibility for this generalized case was proved, and then the design of such transforms was presented as examples.

Next, the preliminaries for the implementation were discussed by introducing the conceptual signal model and the corresponding observer. As a novelty, it was proved that the observer is capable of the realization of the transforms defined in the first half of the article. In particular, this meant that the reconstruction and estimation errors were analyzed, and closed-form expressions were derived for them. To support these claims, the behavior of the observer was explained through an example with emphasis on the interpretation of the state variables.

Lastly, the stability of the observer-based implementation was proved along with the absence of limit cycles and an analysis was given on its computational complexity compared to a naive FIR filter based implementation.

Acknowledgment

The authors acknowledge the financial support of Project No. RRF-2.3.1-21-2022-00009, titled National Laboratory for Renewable Energy that has been implemented with the support provided by the Recovery and Resilience Facility of the European Union within the framework of Széchenyi Plan Plus Program.

References

[1] Allen, J. B., Rabiner, L. R. "A unified approach to short-time Fourier analysis and synthesis", Proceedings of the IEEE, 65(11), pp. 1558–1564, 1977. https://doi.org/10.1109/PROC.1977.10770

[2] Strohmer, T. "Numerical algorithms for discrete Gabor expansions", In: Feichtinger, H. G., Strohmer, T. (eds.) Gabor Analysis and Algorithms: Theory and Applications, Birkhäuser, 1998, pp. 267–291. ISBN 978-1-4612-7382-0 https://doi.org/10.1007/978-1-4612-2016-9_9

[3] Hostetter, G. "Recursive discrete Fourier transformation", IEEE Transactions on Acoustics Speech and Signal Processing, 28(2), pp. 184–190, 1980. https://doi.org/10.1109/tassp.1980.1163389

[4] Péceli, G. "A common structure for recursive discrete transforms", IEEE Transactions on Circuits and Systems, 33(10), pp. 1035–1036, 1986. https://doi.org/10.1109/tcs.1986.1085844

[5] Sujbert, L., Simon, G., Péceli, G. "An Observer-Based Adaptive Fourier Analysis [Tips & Tricks]", IEEE Signal Processing Magazine, 37(4), pp. 134–143, 2020. https://doi.org/10.1109/MSP.2020.2982167

[6] Kollar, Z., Plesznik, F., Trumpf, S. "Observer-Based Recursive Sliding Discrete Fourier Transform [Tips & Tricks]", IEEE Signal Processing Magazine, 35(6), pp. 100–106, 2018. https://doi.org/10.1109/MSP.2018.2853196

[7] Balazs, P., Dörfler, M., Jaillet, F., Holighaus, N., Velasco, G. "Theory, Implementation and Applications of Nonstationary Gabor Frames", Journal of Computational and Applied Mathematics, 236(6), pp. 1481–1496, 2011. https://doi.org/10.1016/j.cam.2011.09.011

[8] Siedenburg, K., Dörfler, M. "Audio denoising by generalized time-frequency thresholding", presented at Audio Engineering Society 45th Conference on Applications of Time-Frequency Processing in Audio, Helsinki, Finland, Mar., 1-4, 2012.

[9] Kovacevic, J., Chebira, A. "Life Beyond Bases: The Advent of Frames (Part I)", IEEE Signal Processing Magazine, 24(4), pp. 86–104, 2007. https://doi.org/10.1109/MSP.2007.4286567

[10] Ország, B., Sujbert, L. "Observer-based discrete Gabor transform", In: 2022 IEEE International Instrumentation and Measurement Technology Conference (I2MTC), Ottawa, ON, Canada, 2022, pp. 1–6. ISBN 978-1-6654-8361-2 https://doi.org/10.1109/I2MTC48687.2022.9806451

[11] Ország, B., Sujbert, L. "Behavior of Observer Performing Discrete Gabor Transform", In: 30th Minisymposium of the Department of Measurement and Information Systems, Budapest, Hungary, 2023, pp. 17–20. ISBN 978-963-421-904-0 https://doi.org/10.3311/minisy2023-005

[12] Vaidyanathan, P., Liu, V. "An improved sufficient condition for absence of limit cycles in digital filters", IEEE Transactions on Circuits and Systems, 34(3), pp. 319–322, 1987. https://doi.org/10.1109/TCS.1987.1086118